

Research Article

Open Access



Reductive O-formylation of carbon dioxide and alcohols over porous phenanthroline-based polymer supported single iridium atom catalyst

Kang Zhao¹, Dongcheng He¹, Hongyan Ni^{1,2}, Hongli Wang¹, Ce Liu¹, Dongyuan Yang³, Xionghou Gao⁴, Junyi Zhang⁴, Honghai Liu⁵, Xinjiang Cui^{1,*}, Feng Shi^{1,*}

¹State Key Laboratory of Low Carbon Catalysis and Carbon Dioxide Utilization, State Key Laboratory for Oxo Synthesis and Selective Oxidation, Lanzhou Institute of Chemical Physics, Chinese Academy of Sciences, Lanzhou 730000, Gansu, China.

²University of Chinese Academy of Sciences, Beijing 100049, China.

³School of Chemistry and Chemical Engineering, Xi'an University of Science and Technology, Xi'an 710054, Shaanxi, China.

⁴PetroChina Lanzhou Petrochemical Company, Lanzhou 730060, Gansu, China.

⁵Petrochina Lanzhou Chemical Research Center, Lanzhou 730060, Gansu, China.

*Correspondence to: Prof. Xinjiang Cui, Prof. Feng Shi, State Key Laboratory of Low Carbon Catalysis and Carbon Dioxide Utilization, State Key Laboratory for Oxo Synthesis and Selective Oxidation, Lanzhou Institute of Chemical Physics, Chinese Academy of Sciences, Lanzhou 730000, Gansu, China. E-mail: xinjiangcui@licp.cas.cn; fshi@licp.cas.cn

How to cite this article: Zhao, K.; He, D.; Ni, H.; Wang, H.; Liu, C.; Yang, D.; Gao, X.; Zhang, J.; Liu, H.; Cui, X.; Shi, F. Reductive O-formylation of carbon dioxide and alcohols over porous phenanthroline-based polymer supported single iridium atom catalyst. *Chem. Synth.* 2025, 5, 75. <https://dx.doi.org/10.20517/cs.2025.13>

Received: 26 Jan 2025 **First Decision:** 13 May 2025 **Revised:** 22 May 2025 **Accepted:** 29 May 2025 **Published:** 15 Sep 2025

Academic Editors: Teng Ben, Giuliano Giambastiani, Tao Zhang **Copy Editor:** Pei-Yun Wang **Production Editor:** Pei-Yun Wang

Abstract

The robust O-formylation of alcohols using carbon dioxide to produce valuable alkyl formats is a green method for achieving carbon capture and utilization. However, developing a highly efficient heterogeneous catalyst with outstanding stability remains a significant challenge. Herein, we report a porous phenanthroline-based polymer-supported single-iridium-atom catalyst (Ir/POP-Phen) for the O-formylation of various alcohols using carbon dioxide and molecular hydrogen. This catalyst demonstrates superior catalytic activity and substrate compatibility compared to previous homogeneous and heterogeneous systems. In the synthesis of bulk methyl formate, the turnover number and turnover frequency reach up to 138,216 and 2,880 h⁻¹, respectively. Additionally, other types of alcohols are successfully converted into their corresponding alkyl formates. Notably, the Ir/POP-Phen catalyst exhibits high tolerance to water concentrations of up to 4,000 ppm during the O-formylation process and can be reused for four cycles without a significant decline in catalytic activity. This work offers insights into the rational design of heterogeneous catalysts for the O-formylation of alcohols.

Keywords: O-formylation, carbon dioxide, porous organic polymer, single iridium atom



© The Author(s) 2025. **Open Access** This article is licensed under a Creative Commons Attribution 4.0 International License (<https://creativecommons.org/licenses/by/4.0/>), which permits unrestricted use, sharing, adaptation, distribution and reproduction in any medium or format, for any purpose, even commercially, as long as you give appropriate credit to the original author(s) and the source, provide a link to the Creative Commons license, and indicate if changes were made.



INTRODUCTION

Since the industrial revolution, anthropogenic carbon dioxide (CO₂) concentrations have risen dramatically from 250 to 415 ppm due to the extensive use of fossil fuels, contributing to global warming, sea-level rise, and extreme weather events^[1,2]. Despite its role as a greenhouse gas, CO₂ represents a nontoxic, abundant, and renewable carbon feedstock. Carbon capture and utilization (CCU) has thus emerged as a critical strategy for mitigating CO₂ emissions while supporting sustainable development in a carbon-constrained economy^[3-6]. In particular, the catalytic conversion of CO₂ into value-added bulk and fine chemicals has garnered significant scientific and industrial interest^[7-11].

Alkyl formates, versatile intermediates in C1 chemistry, are widely used as refrigerants, insecticides, solvents, and platform chemicals for synthesizing formamide, formic acid, and hydrogen energy carriers^[12-15]. The green synthesis of alkyl formates via O-formylation of alcohols with CO₂ and H₂ offers an atom-economical and sustainable pathway, enabling integration with renewable energy systems^[16]. Although homogeneous catalysts such as RuCl₂(dppe)₂ achieve impressive turnover numbers (TONs up to 12,900) and frequencies (TOFs up to 830 h⁻¹) under mild conditions [Supplementary Table 1], their reliance on expensive noble metals, non-recyclable ligands, and poor stability limits practical applications^[17-21]. Heterogeneous catalysts, while addressing recyclability, suffer from inferior activity, metal leaching, and stability issues [Supplementary Table 2]^[22-26]. Additional challenges, including the use of NaBH₄ as a reductant^[27], supercritical CO₂^[12,22,26], high pressures, carbonates instead of CO₂ and H₂ as the substrate^[28], and limited alcohol substrate scope^[29], further hinder its scalability. Thus, developing efficient, stable, and reusable heterogeneous catalysts for O-formylation under environmentally benign conditions remains imperative.

Porous organic polymers (POPs) have recently gained traction as heterogeneous catalytic platforms due to their high surface areas, tunable pore architectures, thermal stability, and tailored functional groups. These properties facilitate the modest adsorption, diffusion, enrichment of chemical molecules and their induced electronic effects during the reaction process^[30,31]. Metal-functionalized POPs have demonstrated exceptional performance in CO₂ transformations, including hydroformylation^[32], O-/N-formylation^[33-36], methanol and formic acid synthesis^[37-39], and cyclic carbonate production^[40,41]. These materials combine the precise control of active metal centers - akin to homogeneous organometallic complexes - with the benefits of heterogeneous systems, such as facile catalyst recovery and recyclability, thereby achieving enhanced reaction performance. For O-formylation, Sun *et al.* developed phosphine-based Ru-POP catalysts^[34], but susceptibility to phosphine oxidation under operational conditions presents a critical limitation. In contrast, nitrogen-ligand-based POPs offer superior oxygen-resistance stability.

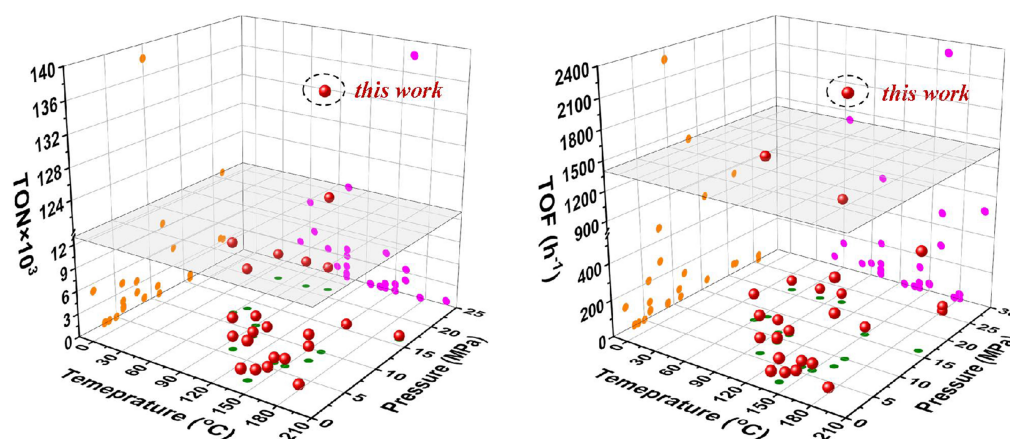
Building on these aforementioned challenges and our long-standing interests in CO₂ valorization and POPs design^[42,43], we report a nitrogen-rich phenanthroline-based porous polymer-supported single-atom iridium catalyst (Ir/POP-Phen) for the O-formylation of diverse alcohols with CO₂ and H₂. This system achieves superior catalytic activity and substrate compatibility, surpassing the precedent work in both homogeneous and heterogeneous catalysis [Figure 1A]. For methyl formate synthesis, TONs of 138,216 and TOFs of 2,880 h⁻¹ were attained [Figure 1B].

EXPERIMENTAL

Preparation of the POP-Phen

First, 0.80 g of 3,8-divinyl-1,10-phenanthroline (2v-Phen) was dissolved in 8 mL of dimethylformamide (DMF), followed by the addition of 20 mg of 2,2'-azobis(2-methylpropionitrile) (AIBN). The mixture was

A. Reaction performance comparison between the precedent and our work



B. This work: O-formylation enabled by the Ir/POP-Phen catalyst

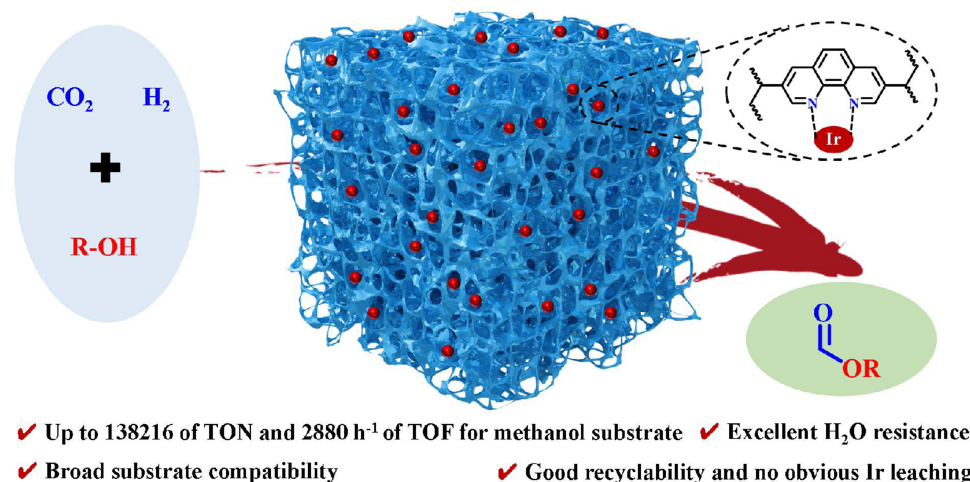


Figure 1. (A) 3D plots based on reaction temperature, reaction pressure [P(CO₂+H₂)], and associated TON or TOF for various reported homo- and heterogeneous catalysts applied for O-formylation of methanol (see [Supplementary Tables 1 and 2](#) for details); (B) O-formylation of alcohols catalyzed by the Ir/POP-Phen catalyst. TON: Turnover number; TOF: turnover frequency; Ir/POP-Phen: porous phenanthroline-based polymer-supported single-iridium-atom catalyst.

transferred into an autoclave, stirred at room temperature for 0.5 h, and then heated to 100 °C for 24 h without stirring. After the polymerization was finished, the resulting solid was filtered, washed with tetrahydrofuran (THF, 20 mL × 3) and Et₂O (20 mL × 3), and dried under vacuum at room temperature. Finally, the POP-Phen was obtained as a yellow solid.

Preparation of the M/POP-Phen

As a typical run, 0.16 g of POP-Phen was swelled in 3 mL of DMF for 1 h, followed by dropwise adding the Ir solution (32 mg of IrCl₃·3H₂O dissolved in 3 mL of DMF) under vigorous stirring. The mixture continued to stir at room temperature for 24 h. After the immobilization of Ir was finished, the resulting solid was filtered, washed with THF (20 mL × 3) and Et₂O (20 mL × 3), and dried under vacuum at room temperature. Finally, the Ir/POP-Phen was obtained as a brown solid. Other kinds of POP-Phen supported metal catalysts were obtained by replacing 32 mg of IrCl₃·3H₂O with 26 mg of Pd(CH₃CN)Cl₂, 26 mg of RhCl₃·3H₂O, 41 mg of H₂PtCl₄, 34 mg of HAuCl₄, 27 mg of RuCl₃·3H₂O, 34 mg of CuCl₂·2H₂O, 24 mg of

$\text{CoCl}_2 \cdot 6\text{H}_2\text{O}$, 17 mg of AgNO_3 , or 24 mg of $\text{NiCl}_2 \cdot 6\text{H}_2\text{O}$, respectively, and denoted as the M/POP-Phen.

Gram-scale preparation of the Ir/POP-Phen

First, 1.6 g of POP-Phen was swelled in 30 mL of DMF for 1 h, followed by dropwise adding the Ir solution (320 mg of $\text{IrCl}_3 \cdot 3\text{H}_2\text{O}$ dissolved in 30 mL of DMF) under vigorous stirring. The mixture continued to stir at room temperature for 24 h. After the immobilization of Ir was finished, the resulting solid was filtered, washed with THF (200 mL \times 3) and Et_2O (200 mL \times 3), and dried under vacuum at room temperature. Finally, the Ir/POP-Phen was obtained as a brown solid.

O-formylation of *n*-BuOH

The as-prepared Ir/POP-Phen catalyst (1.9 mg containing 0.83 μmol of Ir), *n*-BuOH (48 mL), and Et_3N (20 mL) were added into a 140 mL stainless-steel autoclave with a magnetic stir bar. After the autoclave was sealed and purged with 1 MPa of CO_2 four times, the pressure of CO_2 was adjusted to 4 MPa and kept at this pressure for 5 min, then another 6 MPa of H_2 was introduced. So total pressure in the autoclave was 10 MPa at room temperature. The autoclave was put into a preheated reactor, and stirred at 160 $^\circ\text{C}$ for 48 h. After the reaction, the autoclave was cooled to room temperature and the pressure was carefully released. Subsequently, the reaction mixture was diluted with ethyl acetate (8 mL), and the solid catalyst was removed from the system by centrifugation. The liquid was subjected to gas chromatography analysis (Agilent 7890A GC equipped with a HP-5 capillary column with 5 wt.% phenyl groups and the FID detector) to determine the yield, TON, and TOF by using *m*-xylene as the internal standard.

Recycling tests of the Ir/POP-Phen

The as-prepared Ir/POP-Phen catalyst (38 mg containing 16.6 μmol of Ir), *n*-BuOH (48 mL), and Et_3N (20 mL) were added into a 140 mL stainless-steel autoclave with a magnetic stir bar. After the autoclave was sealed and purged with 1 MPa of CO_2 four times, the pressure of CO_2 was adjusted to 4 MPa and kept at this pressure for 5 min, then another 6 MPa of H_2 was introduced. So total pressure in the autoclave was 10 MPa at room temperature. The autoclave was put into a preheated reactor, and stirred at 160 $^\circ\text{C}$ for 12 h. After the reaction, the autoclave was cooled to room temperature and the pressure was carefully released. Subsequently, the reaction mixture was diluted with ethyl acetate (8 mL), and the solid catalyst was removed from the system by centrifugation. The liquid was subjected to gas chromatography analysis (Agilent 7890A GC equipped with a HP-5 capillary column with 5 wt.% phenyl groups and the FID detector) to determine the yield, TON, and TOF by using *m*-xylene as the internal standard.

The spent Ir/POP-Phen catalyst was washed with MeOH (8.0 mL \times 3) and THF (8.0 mL \times 3), and dried at 60 $^\circ\text{C}$ under vacuum. Then the spent Ir/POP-Phen catalyst was used for the next run. The Ir contents of the reused catalyst and filtrate after each run were determined by inductively coupled plasma-atomic emission spectrometry (ICP-AES).

More detailed information, including synthesis methods and materials, is presented in the [Supplementary Materials](#).

RESULTS AND DISCUSSION

Catalyst characterization

The Ir/POP-Phen catalyst was synthesized as follows [Figure 2]: 2v-Phen underwent hydrothermal polymerization at 100 $^\circ\text{C}$ in DMF using AIBN as a radical initiator, yielding the POP-Phen. Subsequently, Ir/POP-Phen was prepared by immobilizing an $\text{IrCl}_3 \cdot \text{H}_2\text{O}$ precursor onto the POP-Phen support via wet impregnation at room temperature. Additional phenanthroline-based polymer-supported metal catalysts were synthesized using analogous protocols [Supplementary Materials].

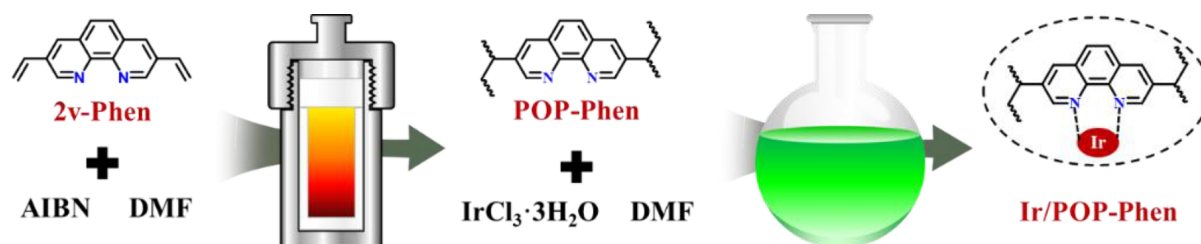


Figure 2. Schematic diagram for the synthesis of the Ir/POP-Phen catalyst. Ir/POP-Phen: Porous phenanthroline-based polymer-supported single-iridium-atom catalyst.

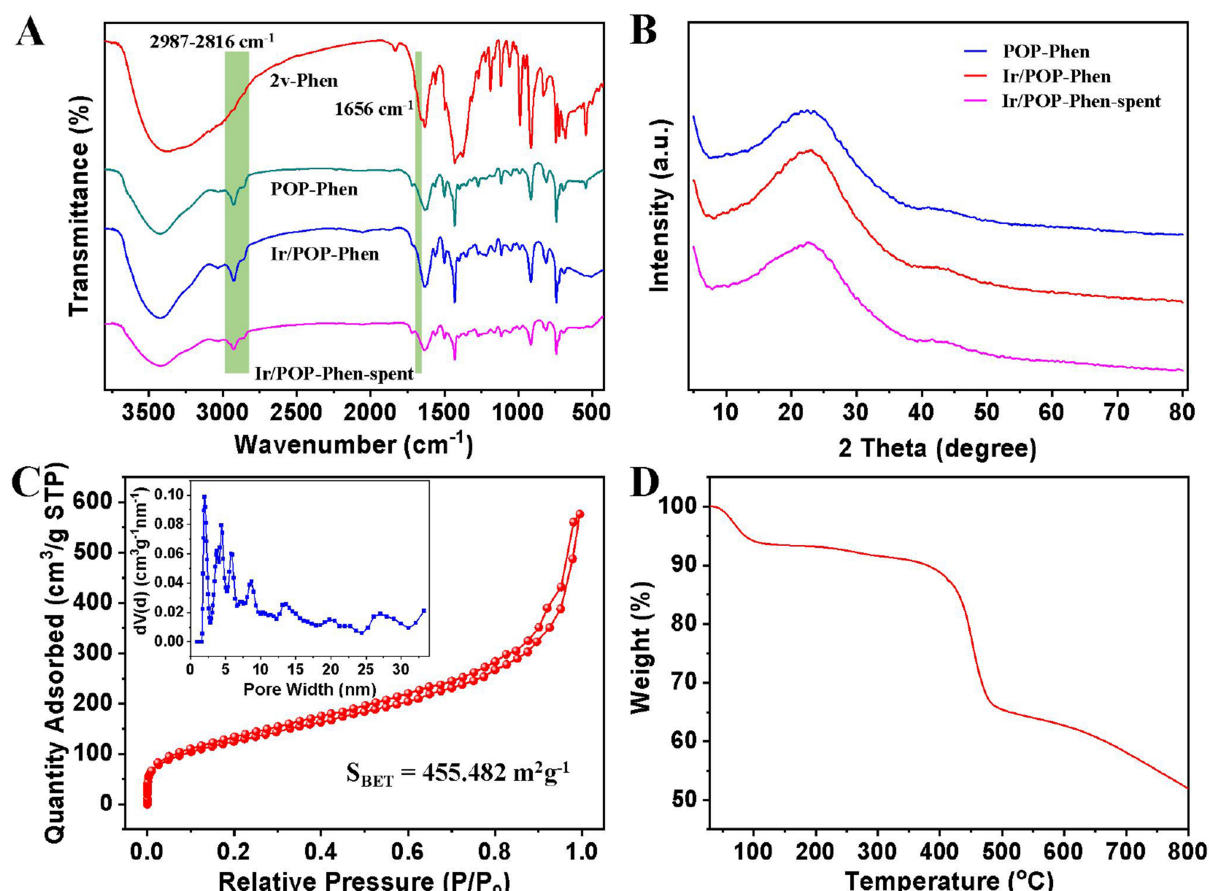


Figure 3. (A) FT-IR spectra of the 2v-Phen, POP-Phen, Ir/POP-Phen, and Ir/POP-Phen-spent; (B) PXRD patterns of the POP-Phen, Ir/POP-Phen, and Ir/POP-Phen-spent; (C) N₂ sorption isotherm, and pore size distribution of the Ir/POP-Phen calculated by NLDFT; (D) TG curve of the Ir/POP-Phen. FT-IR: Fourier-transform infrared; POP-Phen: Ir/POP-Phen: porous phenanthroline-based polymer-supported single-iridium-atom catalyst; NLDFT: nonlocal density functional theory; TG: thermogravimetric.

The catalyst's structure was characterized using multiple techniques. Fourier-transform infrared (FT-IR) spectroscopy [Figure 3A] revealed the disappearance of the vinyl C=C stretching vibration at 1,656 cm⁻¹ in POP-Phen compared to the 2v-Phen monomer, accompanied by new alkyl C-H stretching vibrations at 2,987-2,816 cm⁻¹, confirming successful polymerization. No structural changes were observed in Ir/POP-Phen compared to POP-Phen, indicating that Ir immobilization does not alter the polymer framework. Remarkably, the FT-IR spectrum of the recycled catalyst (Ir/POP-Phen-spent) remained consistent with the fresh catalyst, demonstrating robust chemical stability. Powder X-ray diffraction (PXRD) analysis [Figure

3B] showed no distinct crystalline peaks for POP-Phen or Ir/POP-Phen, confirming the amorphous nature of the polymer and high dispersion of Ir species on the support. The absence of Ir-derived peaks in Ir/POP-Phen-spent further confirmed no metal aggregation during recycling, underscoring the catalyst's structural integrity.

Nitrogen sorption isotherms were conducted to characterize the structural properties of the POP catalysts [Figure 3C, Supplementary Figure 1, and Supplementary Table 3]. For Ir/POP-Phen, a combined Type-I/Type-IV isotherm indicated hierarchical porosity, corroborated by scanning electron microscopy (SEM) and transmission electron microscopy (TEM) imaging [Supplementary Figures 2 and 3]. Nonlocal density functional theory (NLDFT) calculations revealed a predominant pore size distribution of 2–15 nm. Compared to POP-Phen (6.224 nm average pore diameter, 659.420 m²·g⁻¹ BET surface area, 1.026 cm³·g⁻¹ pore volume), Ir/POP-Phen exhibited a larger average pore diameter (7.831 nm) but reduced surface area (455.482 m²·g⁻¹) and pore volume (0.892 cm³·g⁻¹) [Supplementary Table 3]. These changes likely arose from pore expansion induced by Ir species and partial pore occupation during metal loading. Furthermore, the physical properties of Ir/POP-Phen were beneficial for diffusion of the reactants and products. Thermogravimetric (TG) analysis confirmed exceptional thermal stability for Ir/POP-Phen, with decomposition onset near 400 °C [Figure 3D].

For Ir/POP-Phen, layered structure and spherical morphologies were observed by SEM and TEM images [Supplementary Figures 2 and 3]. High-resolution TEM (HR-TEM) showed no Ir nanoclusters [Figure 4A], consistent with X-ray diffraction (XRD) data [Figure 3B], confirming atomic dispersion of Ir on the polymer. Energy-dispersive X-ray (EDX) mapping confirmed uniform distribution of Ir, C, and N [Figure 4B–E], while aberration-corrected high-angle-annular-dark-field scanning transmission electron microscopy (HAADF-STEM) directly visualized single-atom Ir anchored on the polymer [Figure 4F]. *In situ* CO-adsorbed FT-IR spectroscopy [Figure 4G and Supplementary Figure 4] revealed linear Ir(III)-CO stretching vibrations at 2,016 and 1,992 cm⁻¹ after CO exposure, with no bridging CO adsorption, further verifying isolated Ir sites^[44–46]. X-ray absorption near-edge structure (XANES) at the Ir K-edge positioned the Ir oxidation state between 0 and +3 [Figure 4H]. Extended X-ray absorption fine structure (EXAFS) spectra exhibited no Ir–Ir scattering paths [Figure 4I], unambiguously confirming single-atom Ir incorporation. Quantitative EXAFS fitting was performed to elucidate the local coordination environment of Ir in Ir/POP-Phen [Supplementary Table 4 and Supplementary Figure 7]. The analysis revealed two scattering paths at ~2.04 and 2.35 Å, corresponding to Ir–N and Ir–Cl bonds, respectively. These results indicate that a single-atom IrN₄Cl₂ configuration (four Ir–N bonds and two Ir–Cl bonds) dominates the catalytic center of Ir/POP-Phen. Critically, HR-TEM and HAADF-STEM of Ir/POP-Phen-spent [Supplementary Figures 5 and 6] showed no Ir nanoparticle formation, underscoring the catalyst's structural robustness during recycling.

X-ray photoelectron spectroscopy (XPS) was employed to elucidate the chemical state of Ir species and their interaction with the phenanthroline-based polymer [Figure 5]. The Ir 4f binding energy in Ir/POP-Phen appeared at 61.28 eV [Figure 5A], consistent with Ir(III). Notably, this value was 0.3 eV lower than that of the IrCl₃·3H₂O precursor (62.58 eV), indicating electron donation from phenanthroline nitrogen to Ir and confirming coordination between Ir and the polymer backbone^[47]. In addition, compared with the only one peak of N 2p on POP-Phen, the N 2p spectrum of Ir/POP-Phen revealed two distinct peaks at 398.09 and 399.39 eV [Figure 5B], corresponding to free phenanthroline nitrogen and Ir-coordinated phenanthroline nitrogen, respectively. The 1.3 eV upshift in the coordinated nitrogen peak further corroborated electron transfer from nitrogen to Ir, providing direct evidence of metal-ligand interaction. Post-reaction XPS analysis of Ir/POP-Phen-spent showed identical Ir 4f and N 2p profiles to the fresh catalyst [Figure 5C and D], confirming the Ir species retained their +3 oxidation state with no evidence of aggregation during

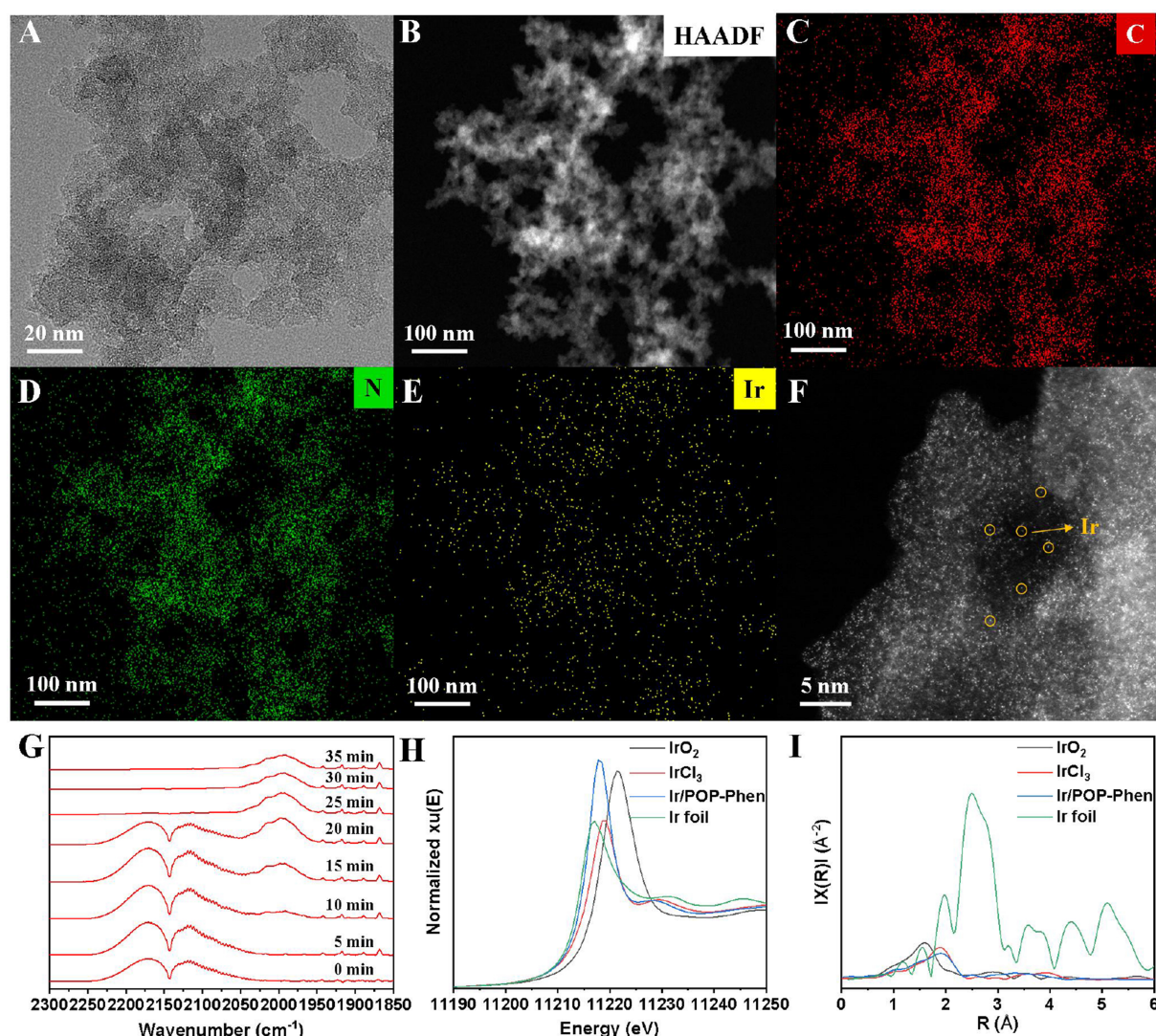


Figure 4. Structural characterization of the Ir/POP-Phen. (A) HR-TEM images of the Ir/POP-Phen; (B-E) EDX elemental mapping of the Ir/POP-Phen; (F) Abreaction-corrected HAADF-STEM image of the Ir/POP-Phen; (G) *In-situ* CO adsorbed FT-IR spectra of the Ir/POP-Phen; (H) XANES spectra of Ir K-edge; (I) EXAFS Fourier transformed spectra. Ir/POP-Phen: Porous phenanthroline-based polymer-supported single-iridium-atom catalyst; HR-TEM: high-resolution-transmission electron microscopy; EDX: energy-dispersive X-ray; HAADF-STEM: high-angle-annular-dark-field scanning transmission electron microscopy; FT-IR: Fourier-transform infrared; XANES: X-ray absorption near-edge structure; EXAFS: extended X-ray absorption fine structure.

catalytic recycling. This aligns with PXRD and HR-TEM data [Figures 3B and 4A], reinforcing the catalyst's structural and electronic stability.

O-formylation application

Optimization of reaction conditions for the O-formylation of *n*-BuOH with CO₂ and H₂ was conducted using Ir/POP-Phen as the catalyst. Initial tests with homogeneous IrCl₃·3H₂O yielded only trace amounts of butyl formate (Table 1, entry 1). Introducing 1,10-phenanthroline (1,10-Phen) as a ligand dramatically enhanced performance, increasing the yield, TON, and TOF to 12.35 mmol, 14,880, and 1,240 h⁻¹, respectively (Table 1, entry 2), attributed to favorable electronic interactions between Ir and 1,10-Phen. To address recyclability of expensive Ir metal and 1,10-Phen ligand, heterogeneous Ir/POP-Phen was synthesized (Table 1, entry 3), achieving superior activity (13.69 mmol yield, 16,494 TON, 1,375 h⁻¹ TOF)

Table 1. Optimization of the catalysts for O-formylation of *n*-BuOH^a

$\text{CO}_2 + \text{H}_2 + n\text{-BuOH} \xrightarrow[160\text{ }^\circ\text{C, 12 h}]{\text{Cat., Et}_3\text{N}} \text{O}-n\text{-Bu}$				
Entry	Cat.	Yield (mmol)	TON	TOF (h ⁻¹)
1	IrCl ₃ ·3H ₂ O	0.32	386	33
2	IrCl ₃ ·3H ₂ O + 1,10-Phen	12.35	14,880	1,240
3	Ir/POP-Phen	13.69	16,494	1,375
4	Ir/POP-Phen-NaBH ₄	2.51	3,019	252
5	Ir@POP-Phen	5.70	6,867	572
6	Ir/POP-Phen&DVB	2.66	3,205	267
7	Ir/POP-Phen& <i>p</i> -3vPA	2.43	2,928	245
8	Ir/POP-Phen ^b	35.50	3,243	30
9	Ir/POP-Phen ^c	1.77	631	53

^aReaction conditions: *n*-BuOH (48 mL, 524 mmol), total pressure (10 MPa) of CO₂ and H₂ (CO₂:H₂ = 4:6), Ir dosage (0.83 μmol), Et₃N (20 mL), reacted at 160 °C for 12 h. Yield, TON, and TOF were determined by GC analysis using *m*-xylene as the internal standard. ^bIr dosage (11 μmol), reacted for 108 h. ^cIr dosage (2.74 μmol), using 4 MPa of flue gas (containing 19.4% of CO₂) instead of pure CO₂ gas. TON: Turnover number; 1,10-Phen: 1,10-phenanthroline hydrate; Ir/POP-Phen: porous phenanthroline-based polymer-supported single-iridium-atom catalyst; DVB: divinylbenzene; TOF: turnover frequency; GC: gas chromatography.

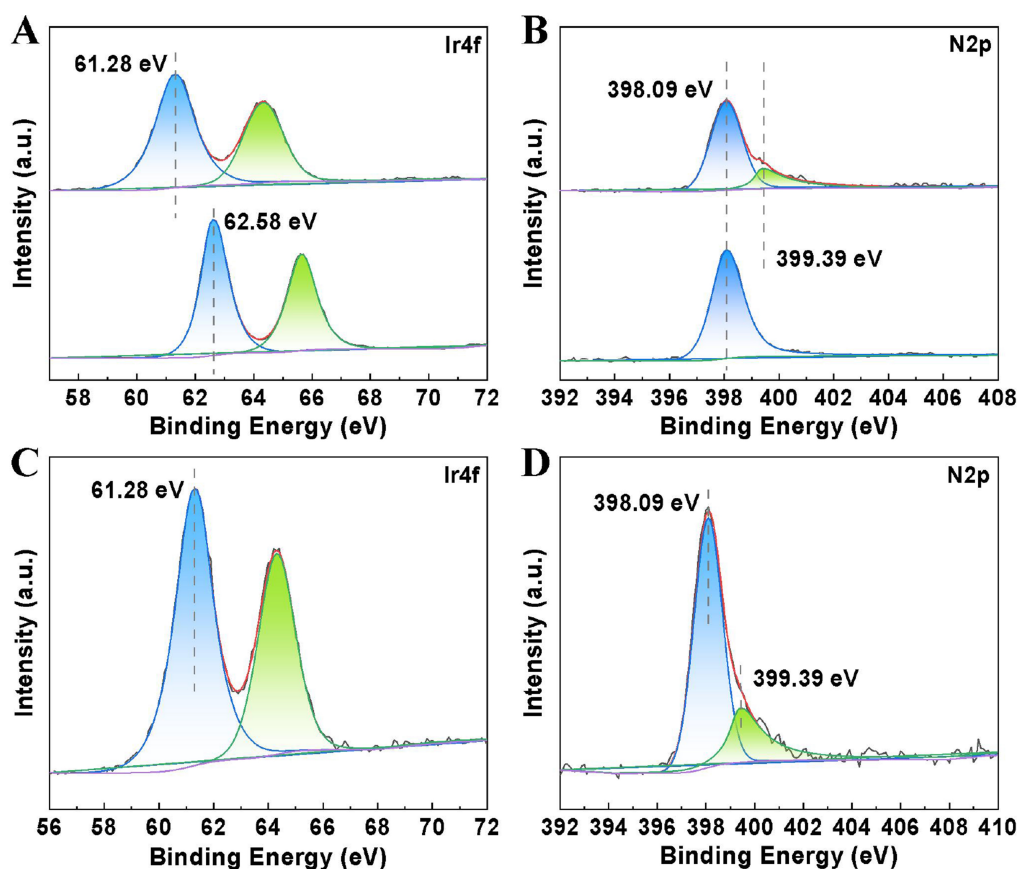


Figure 5. Comparison of the XPS spectra. (A) Biding energy comparison of Ir4f between IrCl₃·3H₂O (bottom) and the Ir/POP-Phen (top); (B) Biding energy comparison of N 2p between POP-Phen (bottom) and the Ir/POP-Phen (top); (C and D) Ir4f and N 2p spectra of the Ir/POP-Phen-spent. XPS: X-ray photoelectron spectroscopy; Ir/POP-Phen: porous phenanthroline-based polymer-supported single-iridium-atom catalyst.

due to enhanced mass transfer via hierarchical porosity and CO₂ activation by pyridinic nitrogen sites on the polymer catalyst. Comparative studies with other metal-loaded POP-Phen catalysts confirmed Ir's superiority [Supplementary Table 5]. Reducing Ir/POP-Phen with NaBH₄ (Ir/POP-Phen-NaBH₄) decreased activity (Table 1, entry 4), likely due to Ir nanoparticle formation and reduced active site accessibility. The *in situ* encapsulated Ir species within the POP (Ir@POP-Phen) was synthesized via one-pot solvothermal polymerization. When tested in the O-formylation reaction, Ir@POP-Phen achieved a TON of 6,867 and a TOF of 572 h⁻¹ (Table 1, entry 5). Other types of heterogeneous Ir catalysts, prepared by copolymerizing 1,10-Phen with divinylbenzene (DVB) or tris(4-vinylphenyl)amine (*p*-3vPA), were evaluated (Table 1, entries 6 and 7). However, these systems underperformed compared to the optimized Ir/POP-Phen, attributed to reduced 1,10-Phen ligand density in the polymer matrices. Scaling Ir loading to 11 μmol and extending reaction time to 108 h boosted the yield to 35.5 mmol (Table 1, entry 8). Remarkably, Ir/POP-Phen enabled direct CO₂ utilization from industrial flue gas (19.4% CO₂), achieving 1.77 mmol yield, 631 TON, and 53 h⁻¹ TOF (Table 1, entry 9).

Subsequently, other key reaction parameters for the O-formylation were optimized. Increasing the Ir loading enhanced the butyl formate yield incrementally until it plateaued at 16.60 μmol of Ir [Figure 6A]. However, both TON and TOF declined markedly, indicating a reduced reaction rate at higher Ir loadings. Peak TON and TOF values were achieved at an Ir loading of 0.83 μmol. A volcano-shaped trend emerged with rising reaction temperature (140–180 °C), with 160 °C identified as optimal [Figure 6B]. Systematic evaluation of CO₂ and H₂ pressures, alongside organic base screening, revealed 4 MPa CO₂, 6 MPa H₂, and cost-effective Et₃N as ideal conditions [Figure 6C and D].

Furthermore, the amounts of *n*-BuOH and Et₃N were optimized, identifying 48 mL of *n*-BuOH and 20 mL of Et₃N as the optimal conditions [Figure 7A and B]. The O-formylation reaction produces H₂O as a by-product, whose accumulation can perturb the reaction equilibrium and diminish catalytic efficiency^[29]. Consequently, evaluating the impact of H₂O concentration on performance was critical. Remarkably, the Ir/POP-Phen catalyst exhibited robust activity even at H₂O concentrations up to 4,000 ppm, underscoring its exceptional water tolerance [Figure 7C].

A kinetic study was conducted to elucidate the relationship between reaction performance and time [Figure 7D and E]. The results revealed that the yield and TON increased progressively, peaking at 21.38 mmol and 25,759, respectively, after 48 h. In contrast, the TOF rose initially (≤ 3 h) but declined thereafter, reflecting a deceleration in product formation over time. Moreover, a hot filtration experiment was performed to confirm the catalyst's stability [Figure 7E], and 8.74 mmol of butyl formate was generated within the initial 6 h using Ir/POP-Phen. After catalyst removal, the filtrate showed no further yield increase over 42 additional hours, confirming negligible homogeneous catalysis. ICP-AES analysis of the filtrate detected no Ir leaching (< 0.1 ppm), validating the heterogeneous nature of the catalytic system. Following, the Ir/POP-Phen catalyst was reused four times via centrifugation and drying, retaining its activity [Figure 7F]. Consistent Ir loadings of the catalysts (8.30 wt.% for fresh vs. 8.13–8.31 wt.% for recycled catalysts) and undetectable Ir leaching (< 0.1 ppm) in the filtrate during all cycles [Supplementary Table 6] underscored exceptional stability, attributed to strong coordinative Ir–phenanthroline nitrogen interactions within the polymer framework.

Substrate compatibility was systematically investigated to evaluate the universality of Ir/POP-Phen, addressing a notable gap in prior studies of alcohol scope for O-formylation^[14,48]. The catalyst demonstrated exceptional performance in synthesizing bulk industrial chemicals: methyl formate (114.72 mmol yield, TON = 138,216, TOF = 2,880 h⁻¹) and ethyl formate (33.28 mmol yield, TON = 40,096, TOF = 835 h⁻¹) were

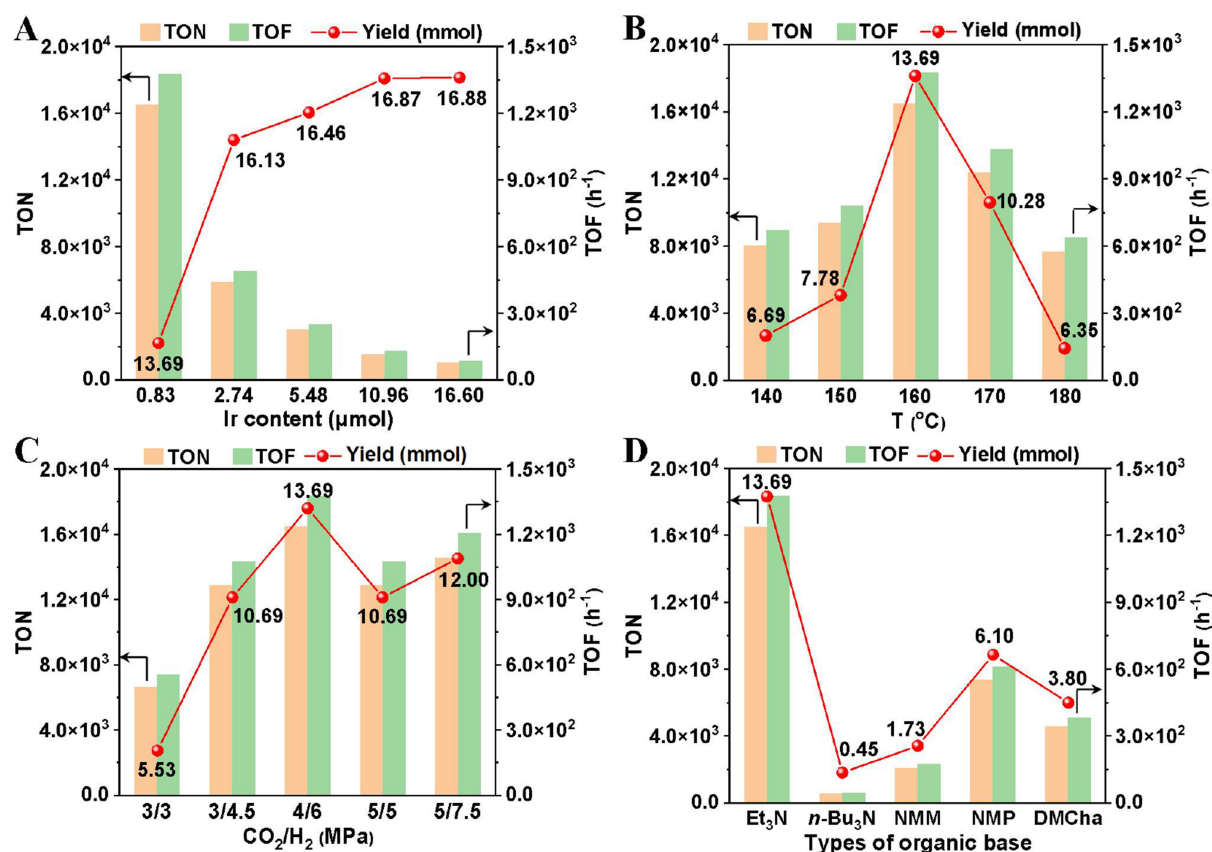


Figure 6. Optimization of the reaction conditions. General reaction conditions: *n*-BuOH (48 mL, 524 mmol), total pressure (10 MPa) of CO₂ and H₂ (CO₂:H₂ = 4:6), Ir dosage (0.83 μmol), Et₃N (20 mL), reacted at 160 °C for 12 h. Yield, TON, and TOF were determined by GC analysis using *m*-xylene as the internal standard. (A) Screening of the Ir dosage of the Ir/POP-Phen; (B) Screening of the reaction temperature; (C) Screening of the pressure of CO₂ and H₂; (D) Screening of the organic bases. TON: Turnover number; TOF: turnover frequency; GC: gas chromatography; Ir/POP-Phen: porous phenanthroline-based polymer-supported single-iridium-atom catalyst; NMM: 4-methylmorpholine, NMP: 1-methylpyrrolidine, DMCha: N, N-dimethylcyclohexylamine.

produced efficiently from O-formylation of methanol and ethanol, respectively (Table 2, entries 1 and 2). Long-chain aliphatic alcohols (Table 2, entries 3-5) and sterically hindered alcohols (Table 2, entries 6 and 7) exhibited reduced activity, likely due to pore size limitations restricting diffusion of bulky molecules. Notably, benzyl formate - a key flavoring agent and solvent in the fragrance industry^[49] - was synthesized from O-formylation of benzyl alcohol with high efficiency (Table 2, entry 8), highlighting the catalyst's versatility.

Mechanism discussion

Building on experimental results and prior mechanistic studies^[33,34,50,51], a plausible reaction mechanism for alkyl formate synthesis over Ir/POP-Phen is proposed [Figure 8]. The catalytic cycle initiates with H₂ dissociation at the phenanthroline-coordinated Ir complex (I), while free phenanthroline sites adsorb and activate CO₂. This generates an Ir-hydride intermediate (II), a recognized prerequisite for CO₂ hydrogenation. Subsequent CO₂ insertion into the Ir-H bond forms a metal-bound formate species (III). Reductive elimination between the Ir-hydride and Ir-formate of III releases formic acid, regenerating the active Ir complex (I). The liberated formic acid is trapped by Et₃N, forming a HCOO·Et₃NH⁺ ion pair, which undergoes esterification with alcohols to yield alkyl formates, releasing Et₃N for subsequent cycles.

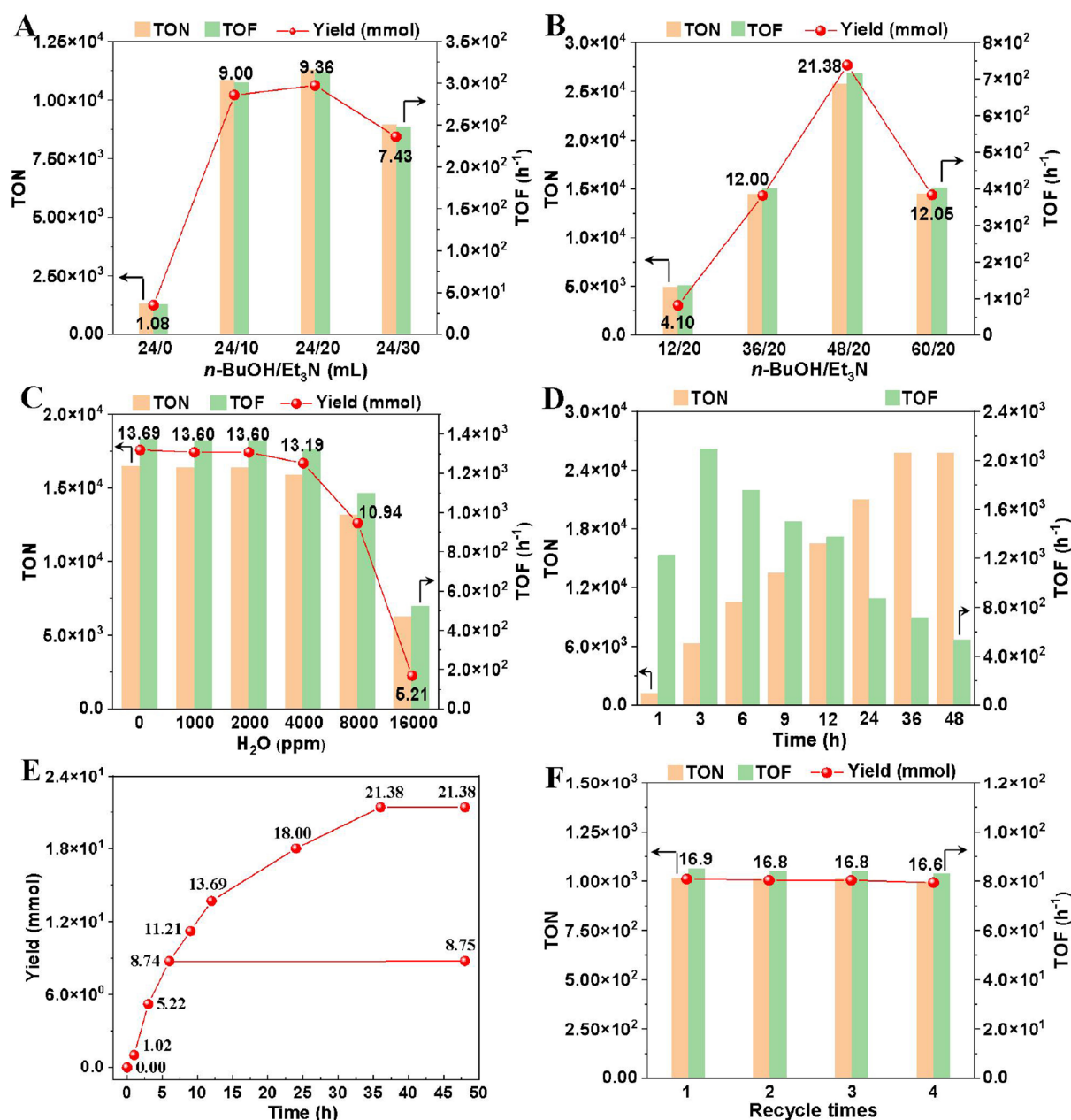

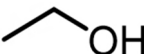


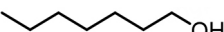
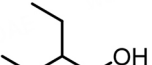
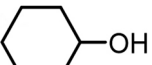
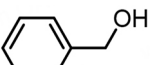


Figure 7. Optimization of other reaction parameters and recycle tests of the Ir/POP-Phen. General reaction conditions: *n*-BuOH (48 mL, 524 mmol), total pressure (10 MPa) of CO₂ and H₂ (CO₂:H₂ = 4:6), Ir dosage (0.83 μmol), Et₃N (20 mL), reacted at 160 °C for 12 h. Yield, TON, and TOF were determined by GC analysis using *m*-xylene as the internal standard. (A and B) Screening of the amount of *n*-BuOH and Et₃N; (C) Screening of the amount of H₂O added; (D and E) Kinetic study and hot-filtration experiments; (F) Recyclability of the Ir/POP-Phen. Ir/POP-Phen: Porous phenanthroline-based polymer-supported single-iridium-atom catalyst; TON: turnover number; TOF: turnover frequency; GC: gas chromatography.

CONCLUSIONS

In summary, a single-atom iridium catalyst supported on a phenanthroline-based POP (Ir/POP-Phen) was successfully developed for the synthesis of value-added alkyl formates via O-formylation of diverse alcohols using CO₂ and H₂ as feedstocks. The catalyst demonstrated excellent activity and broad substrate scope, achieving unprecedented TONs (TON = 138,216) and frequencies (TOF = 2,880 h⁻¹) for methyl formate synthesis - surpassing those of previously reported homogeneous and heterogeneous catalytic systems.

Table 2. Substrate scope for O-formylation^a

$\text{CO}_2 + \text{H}_2 + \text{R-OH} \xrightarrow[160\text{ }^\circ\text{C, 48 h}]{\text{Ir/POP-Phen, Et}_3\text{N}} \text{O-C(=O)-OR}$				
Entry	Substrate	Yield (mmol)	TON	TOF (h ⁻¹)
1		114.72	138,216	2,880
2		33.28	40,096	835
3		17.31	20,855	434
4		21.38	25,759	536
5		6.33	7,627	159
6		7.11	8,567	179
7		5.35	6,446	135
8		5.35	6,446	135

^aReaction conditions: alcohols (48 mL), total pressure (10 MPa) of CO₂ and H₂ (CO₂:H₂ = 4:6), Ir/POP-Phen (1.9 mg, 0.83 μmol), Et₃N (20 mL), reacted at 160 °C for 48 h. Yield, TON, and TOF for MeOH and *n*-BuOH were determined by GC analysis using *m*-xylene as the internal standard, while those for other alcohols were determined by ¹H NMR analysis using 1,3,5-trimethoxybenzene as the internal standard. TON: Turnover number; TOF: turnover frequency; Ir/POP-Phen: porous phenanthroline-based polymer-supported single-iridium-atom catalyst; GC: gas chromatography; NMR: nuclear magnetic resonance.

Notably, Ir/POP-Phen exhibited robust performance even at H₂O concentrations up to 4,000 ppm, highlighting its practical potential under industrially relevant conditions. Recycling tests confirmed outstanding stability, with no significant activity loss or Ir leaching (< 0.1 ppm) observed over multiple cycles. Comprehensive characterization (FT-IR, PXRD, N₂ sorption, TGA, SEM, TEM, XPS) validated the catalyst's structural integrity and single-atom Ir coordination. This work advances the rational design of POP-based catalysts for CO₂ valorization and provides a viable strategy for enhancing carbon CCU efficiency in chemical manufacturing.

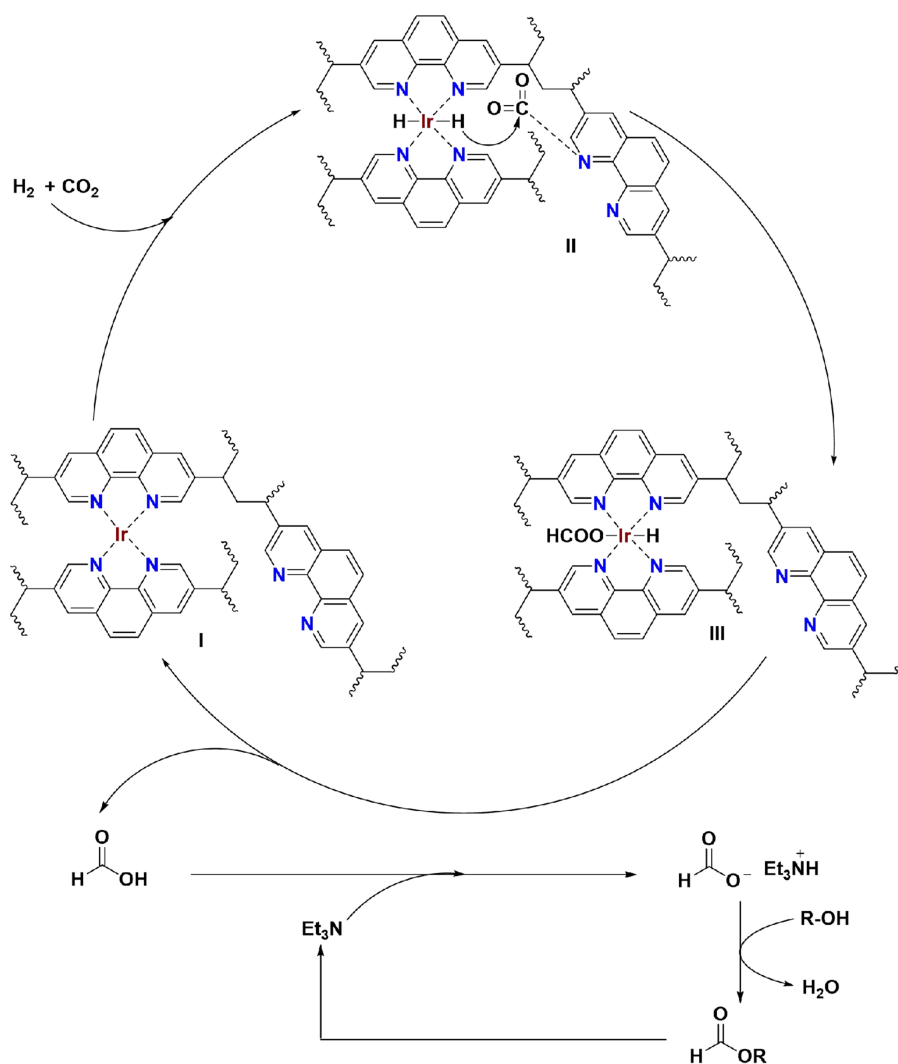


Figure 8. Proposed catalytic cycle.

DECLARATIONS

Authors' contributions

Developed the project: Shi, F.; Cui, X.

Designed and performed most of the experiments and data analysis: Zhao, K.

Participated in part of the experiments: He, D.; Ni, H.; Wang, H.; Liu, C.; Yang, D.; Gao, X.; Zhang, J.; Liu, H.

Supervised the project: Cui, X.; Shi, F.

Prepared a manuscript draft: Zhao, K.

Contributed to the final manuscript: Cui, X.; Shi, F.

Availability of data and materials

The detailed materials and methods in the experiment were listed in the [Supplementary Materials](#). Other raw data that support the findings of this study are available from the corresponding author upon reasonable request.

Financial support and sponsorship

This study was supported by the National Natural Science Foundation of China (U22A20393, 22372180, 22402212 and 22202216), the Natural Science Foundation of Gansu Province (25JRRA473), the PetroChina Lanzhou Petrochemical Company (LZSH-2025-JS-14), CAS Project for Young Scientists in Basic Research (Grant No. YSBR-050), the Major Project of Gansu Province (21ZD4WA021, 22ZD6GA003 and 23ZDFA016), the Science and Technology Planning Project of Lanzhou City (2023-1-15), and International Partnership Program of Chinese Academy of Sciences (037GJHZ2023010FN).

Conflicts of interest

Gao, X. and Zhang, J. are affiliated with PetroChina Lanzhou Petrochemical Company. Liu, H. is affiliated with PetroChina Lanzhou Chemical Research Center. The other authors declared that there are no conflicts of interest.

Ethical approval and consent to participate

Not applicable.

Consent for publication

Not applicable.

Copyright

© The Author(s) 2025.

REFERENCES

1. Álvarez, A.; Bansode, A.; Urakawa, A.; et al. Challenges in the greener production of formates/formic acid, methanol, and DME by heterogeneously catalyzed CO₂ hydrogenation processes. *Chem. Rev.* **2017**, *117*, 9804-38. DOI PubMed PMC
2. Sun, R.; Liao, Y.; Bai, S.; et al. Heterogeneous catalysts for CO₂ hydrogenation to formic acid/formate: from nanoscale to single atom. *Energy. Environ. Sci.* **2021**, *14*, 1247-85. DOI
3. Mac Dowell, N.; Fennell, P. S.; Shah, N.; Maitland, G. C. The role of CO₂ capture and utilization in mitigating climate change. *Nature. Clim. Change.* **2017**, *7*, 243-9. DOI
4. Ramirez, A.; Gong, X.; Caglayan, M.; et al. Selectivity descriptors for the direct hydrogenation of CO₂ to hydrocarbons during zeolite-mediated bifunctional catalysis. *Nat. Commun.* **2021**, *12*, 5914. DOI PubMed PMC
5. Li, N.; Zhang, X.; Shi, M.; Zhou, S. The prospects of China's long-term economic development and CO₂ emissions under fossil fuel supply constraints. *Resour. Conserv. Recycl.* **2017**, *121*, 11-22. DOI
6. Mardani, A.; Streimikiene, D.; Cavallaro, F.; Loganathan, N.; Khoshnoudi, M. Carbon dioxide (CO₂) emissions and economic growth: a systematic review of two decades of research from 1995 to 2017. *Sci. Total. Environ.* **2019**, *649*, 31-49. DOI PubMed
7. Guan, C.; Pan, Y.; Ang, E. P. L.; et al. Conversion of CO₂ from air into formate using amines and phosphorus-nitrogen PN³P-Ru(II) pincer complexes. *Green. Chem.* **2018**, *20*, 4201-5. DOI
8. Jiang, X.; Nie, X.; Guo, X.; Song, C.; Chen, J. G. Recent advances in carbon dioxide hydrogenation to methanol via heterogeneous catalysis. *Chem. Rev.* **2020**, *120*, 7984-8034. DOI
9. Liang, H. Q.; Beweries, T.; Francke, R.; Beller, M. Molecular catalysts for the reductive homocoupling of CO₂ towards C₂₊ compounds. *Angew. Chem. Int. Ed. Engl.* **2022**, *61*, e202200723. DOI PubMed PMC
10. Zhao, S.; Liang, H. Q.; Hu, X. M.; Li, S.; Daasbjerg, K. Challenges and prospects in the catalytic conversion of carbon dioxide to formaldehyde. *Angew. Chem. Int. Ed. Engl.* **2022**, *61*, e202204008. DOI PubMed PMC
11. Wang, D.; Sun, X.; Yin, H.; Dong, H.; Liu, H.; Zhang, Y. Tuning selectivity of CO₂ hydrogenation via support composition modification adjusted the activity reduction of H species over Ce_{1-x}Pr_xO_{2-δ}-supported metal (Ru, Rh) nanoclusters. *ACS. Catal.* **2024**, *14*, 10060-76. DOI
12. Jessop, P. G.; Hsiao, Y.; Ikariya, T.; Noyori, R. Homogeneous catalysis in supercritical fluids: hydrogenation of supercritical carbon dioxide to formic acid, alkyl formates, and formamides. *J. Am. Chem. Soc.* **1996**, *118*, 344-55. DOI
13. Federsel, C.; Boddien, A.; Jackstell, R.; et al. A well-defined iron catalyst for the reduction of bicarbonates and carbon dioxide to formates, alkyl formates, and formamides. *Angew. Chem. Int. Ed. Engl.* **2010**, *49*, 9777-80. DOI PubMed
14. Lemmens, V.; Vanbergen, T.; O'Rourke, G.; Marquez, C.; De Vos, D. E. Cascade catalysis for the hydrogenation of carbon dioxide to methyl formate using a molecular Ru-phosphine complex and the metal-organic framework UiO-66 as heterogeneous acid. *ACS. Appl. Energy. Mater.* **2023**, *6*, 9153-8. DOI
15. Sang, R.; Wei, Z.; Hu, Y.; et al. Methyl formate as a hydrogen energy carrier. *Nat. Catal.* **2023**, *6*, 543-50. DOI
16. Scott, M.; Westhues, C. G.; Kaiser, T.; et al. Methylformate from CO₂: an integrated process combining catalytic hydrogenation and reactive distillation. *Green. Chem.* **2019**, *21*, 6307-17. DOI

17. Kröcher, O.; Köppel, R. A.; Baiker, A. Highly active ruthenium complexes with bidentate phosphine ligands for the solvent-free catalytic synthesis of N,N-dimethylformamide and methyl formate. *Chem. Commun.* **1997**, 453-4. DOI
18. Darensbourg, D. J.; Ovalles, C.; Pala, M. Homogeneous catalysts for carbon dioxide/hydrogen activation. Alkyl formate production using anionic ruthenium carbonyl clusters as catalysts. *J. Am. Chem. Soc.* **1983**, *105*, 5937-9. DOI
19. Ziebart, C.; Federsel, C.; Anbarasan, P.; et al. Well-defined iron catalyst for improved hydrogenation of carbon dioxide and bicarbonate. *J. Am. Chem. Soc.* **2012**, *134*, 20701-4. DOI
20. Gowrisankar, S.; Federsel, C.; Neumann, H.; et al. Synthesis of stable phosphonide ligands and their use in Ru-catalyzed hydrogenations of bicarbonate and related substrates. *ChemSusChem* **2013**, *6*, 85-91. DOI
21. Westhues, N.; Belleflamme, M.; Klankermayer, J. Base-free hydrogenation of carbon dioxide to methyl formate with a molecular ruthenium-phosphine catalyst. *ChemCatChem* **2019**, *11*, 5269-74. DOI
22. Yu, K. M.; Yeung, C. M.; Tsang, S. C. Carbon dioxide fixation into chemicals (methyl formate) at high yields by surface coupling over a Pd/Cu/ZnO nanocatalyst. *J. Am. Chem. Soc.* **2007**, *129*, 6360-1. DOI
23. Wu, C.; Zhang, Z.; Zhu, Q.; Han, H.; Yang, Y.; Han, B. Highly efficient hydrogenation of carbon dioxide to methyl formate over supported gold catalysts. *Green. Chem.* **2015**, *17*, 1467-72. DOI
24. Ayodele, O. B.; Tasfy, S. F. H.; Zabidi, N. A. M.; Uemura, Y. Co-synthesis of methanol and methyl formate from CO₂ hydrogenation over oxalate ligand functionalized ZSM-5 supported Cu/ZnO catalyst. *J. CO₂ Util.* **2017**, *17*, 273-83. DOI
25. Corral-Pérez, J. J.; Bansode, A.; Praveen, C. S.; et al. Decisive role of perimeter sites in silica-supported Ag nanoparticles in selective hydrogenation of CO₂ to methyl formate in the presence of methanol. *J. Am. Chem. Soc.* **2018**, *140*, 13884-91. DOI PubMed
26. Corral-Pérez, J. J.; Copéret, C.; Urakawa, A. Lewis acidic supports promote the selective hydrogenation of carbon dioxide to methyl formate in the presence of methanol over Ag catalysts. *J. Catal.* **2019**, *380*, 153-60. DOI
27. Gastelu, G.; Savary, D.; Hulla, M.; Ortiz, D.; Uranga, J. G.; Dyson, P. J. Autocatalytic O-formylation of alcohols using CO₂. *ACS. Catal.* **2023**, *13*, 2403-9. DOI
28. Federsel, C.; Ziebart, C.; Jackstell, R.; Baumann, W.; Beller, M. Catalytic hydrogenation of carbon dioxide and bicarbonates with a well-defined cobalt dihydrogen complex. *Chemistry* **2012**, *18*, 72-5. DOI PubMed
29. Kerry Yu, K. M.; Tsang, S. C. A study of methyl formate production from carbon dioxide hydrogenation in methanol over a copper zinc oxide catalyst. *Catal. Lett.* **2011**, *141*, 259-65. DOI
30. Kramer, S.; Bennedsen, N. R.; Kegnæs, S. Porous organic polymers containing active metal centers as catalysts for synthetic organic chemistry. *ACS. Catal.* **2018**, *8*, 6961-82. DOI
31. Song, K. S.; Fritz, P. W.; Coskun, A. Porous organic polymers for CO₂ capture, separation and conversion. *Chem. Soc. Rev.* **2022**, *51*, 9831-52. DOI PubMed PMC
32. Wang, G.; Jiang, M.; Sun, Z.; et al. Synergistic effect between monophosphine species for regioselective hydroformylation of olefin with CO₂. *Chem. Eng. J.* **2023**, *476*, 146332. DOI
33. Corral-Pérez, J. J.; Billings, A.; Stoian, D.; Urakawa, A. Continuous hydrogenation of carbon dioxide to formic acid and methyl formate by a molecular iridium complex stably heterogenized on a covalent triazine framework. *ChemCatChem* **2019**, *11*, 4725-30. DOI
34. Sun, R.; Kann, A.; Hartmann, H.; Besmehn, A.; Hausoul, P. J. C.; Palkovits, R. Direct synthesis of methyl formate from CO₂ with phosphine-based polymer-bound Ru catalysts. *ChemSusChem* **2019**, *12*, 3278-85. DOI PubMed
35. Wang, G.; Jiang, M.; Ji, G.; et al. Bifunctional heterogeneous Ru/POP catalyst embedded with alkali for the N-formylation of amine and CO₂. *ACS. Sustainable. Chem. Eng.* **2020**, *8*, 5576-83. DOI
36. Shen, Y.; Zheng, Q.; Chen, Z. N.; et al. Highly efficient and selective N-formylation of amines with CO₂ and H₂ catalyzed by porous organometallic polymers. *Angew. Chem. Int. Ed. Engl.* **2021**, *60*, 4125-32. DOI
37. Hlathshwayo, Z. T.; Doremus, J. G.; McGrier, P. L. Hydrosilylative reduction of CO₂ to formate and methanol using a cobalt porphyrin-based porous organic polymer. *ChemCatChem* **2022**, *14*, e202200783. DOI
38. Zhang, Z.; Zhang, L.; Yao, S.; et al. Support-dependent rate-determining step of CO₂ hydrogenation to formic acid on metal oxide supported Pd catalysts. *J. Catal.* **2019**, *376*, 57-67. DOI
39. Ma, W.; Xiong, W.; Hu, J.; Geng, J.; Hu, X. Highly efficient catalysts for CO₂ hydrogenation to formic acid in water catalyzed by hydrophobic porous polymers containing stable metal-hydride. *Green. Chem.* **2024**, *26*, 4192-8. DOI
40. Wang, W.; Li, C.; Yan, L.; Wang, Y.; Jiang, M.; Ding, Y. Ionic liquid/Zn-PPh₃ integrated porous organic polymers featuring multifunctional sites: highly active heterogeneous catalyst for cooperative conversion of CO₂ to cyclic carbonates. *ACS. Catal.* **2016**, *6*, 6091-100. DOI
41. Wang, W.; Wang, Y.; Li, C.; Yan, L.; Jiang, M.; Ding, Y. State-of-the-art multifunctional heterogeneous POP catalyst for cooperative transformation of CO₂ to cyclic carbonates. *ACS. Sustainable. Chem. Eng.* **2017**, *5*, 4523-8. DOI
42. Wu, Y.; Wang, T.; Wang, H.; Wang, X.; Dai, X.; Shi, F. Active catalyst construction for CO₂ recycling via catalytic synthesis of N-doped carbon on supported Cu. *Nat. Commun.* **2019**, *10*, 2599. DOI PubMed PMC
43. Zhao, K.; Wang, H.; Wang, X.; et al. Confinement of atomically dispersed Rh catalysts within porous monophosphine polymers for regioselective hydroformylation of alkenes. *J. Catal.* **2021**, *401*, 321-30. DOI
44. Lu, Y.; Wang, J.; Yu, L.; et al. Identification of the active complex for CO oxidation over single-atom Ir-on-MgAl₂O₄ catalysts. *Nat. Catal.* **2019**, *2*, 149-56. DOI
45. Cheng, D.; Wang, M.; Tang, L.; et al. Catalytic synthesis of formamides by integrating CO₂ capture and morpholine formylation on

- supported iridium catalyst. *Angew. Chem. Int. Ed. Engl.* **2022**, *61*, e202202654. DOI PubMed
46. Wei, X.; Zhang, X.; Jiang, Y.; et al. Ionic liquid boosting N-formylation of amines on polyoxometalate-stabilizing iridium single-atom catalysts. *J. Catal.* **2024**, *433*, 115493. DOI
 47. Gunasekar, G. H.; Yoon, S. A phenanthroline-based porous organic polymer for the iridium-catalyzed hydrogenation of carbon dioxide to formate. *J. Mater. Chem. A* **2019**, *7*, 14019-26. DOI
 48. Yadav, M.; Linehan, J. C.; Karkamkar, A. J.; van der Eide, E.; Heldebrant, D. J. Homogeneous hydrogenation of CO₂ to methyl formate utilizing switchable ionic liquids. *Inorg. Chem.* **2014**, *53*, 9849-54. DOI PubMed
 49. Sá, A. G. A.; Meneses, A. C. D.; Araújo, P. H. H. D.; Oliveira, D. D. A review on enzymatic synthesis of aromatic esters used as flavor ingredients for food, cosmetics and pharmaceuticals industries. *Trends. Food. Sci. Technol.* **2017**, *69*, 95-105. DOI
 50. Lee, B.; Gong, E.; Kim, M.; et al. Electronic interaction between transition metal single-atoms and anatase TiO₂ boosts CO₂ photoreduction with H₂O. *Energy. Environ. Sci.* **2022**, *15*, 601-9. DOI
 51. Ma, J.; Lee, W.; Kim, J. H.; et al. Leveraging the intermetal distance in dual-atom catalysts: revealing optimized synergistic interactions for CO₂ electroreduction. *ACS. Nano.* **2025**, *19*, 18698-707. DOI